ACS OMEGA

http://pubs.acs.org/journal/acsodf

Article

Chemical Activation and Mechanical Sensitization of Piezo1 Enhance TRAIL-Mediated Apoptosis in Glioblastoma Cells

Samantha V. Knoblauch, Shanay H. Desai, Jenna A. Dombroski, Nicole S. Sarna, Jacob M. Hope, and Michael R. King*

Cite This: *ACS Omega* 2023, 8, 16975−16986

Read Online

ACCESS | Metrics & More | Article Recommendations | Supporting Information

ABSTRACT: Glioblastoma multiforme (GBM), the most common and aggressive type of primary brain tumor, has a mean survival of less than 15 months after standard treatment. Treatment with the current standard of care, temozolomide (TMZ), may be ineffective if damaged tumor cells undergo DNA repair or acquire mutations that inactivate transcription factor p53. Tumor necrosis factor-related apoptosis-inducing ligand (TRAIL) triggers apoptosis in multiple tumor types, while evading healthy cells, through a transcription-independent mechanism. GBM is particularly resistant to TRAIL, but studies have found that the mechanoreceptor Piezo1 can be activated under static conditions via Yoda1 agonist to induce TRAIL sensitization in other cancer cell lines. This study examines the effects and the mechanism of chemical and mechanical activation of Piezo1, via Yoda1 and fluid shear stress (FSS) stimulation, on TRAIL-mediated apoptosis in GBM cells. Here, we demonstrate that Yoda1 + TRAIL and FSS + TRAIL combination therapies significantly increase apoptosis in two GBM cell lines relative to controls. Further, cells known to be resistant to TMZ were found to have higher levels of Piezo1 expression and were more susceptible to TRAIL sensitization by Piezo1 activation. The combinatory Yoda1 + TRAIL treatment significantly decreased cell viability in TMZ-resistant GBM cells when compared to treatment with both low and high doses of TMZ. The results of this study suggest the potential of a highly specific and minimally invasive approach to overcome TMZ resistance in GBM by sensitizing cancer cells to TRAIL treatment via chemical or mechanical activation of Piezo1.

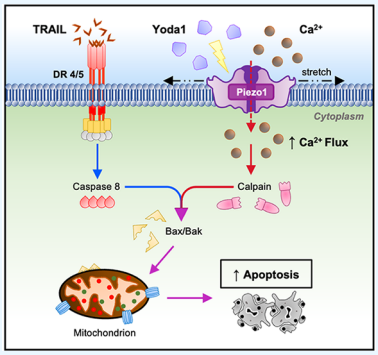

INTRODUCTION

Glioblastoma multiforme (GBM), the most aggressive adult central nervous system tumor, is associated with one of the worst mortality rates of all cancers and is generally regarded as incurable.[1−3] The standard treatment route for this aggressive disease is maximal safe tumor resection followed by systemic chemotherapy with temozolomide (TMZ) and local radiotherapy to initiate cellular apoptosis in remaining cancer cells by damaging their DNA.[1,4−7] This standard therapy has significantly extended the lifetime of glioblastoma patients.[8] However, the mean survival post-treatment is only 14 to 15 months, with just 10% of patients surviving at least 5 years post-diagnosis.[1,8]

The invasive nature of GBM and the biological heterogeneity of its cells make complete eradication of cancer cells difficult with the standard treatment, leading to poor patient outcomes.[2,3,8] There is also no standard therapy outlined for tumor recurrence post-surgery despite 80% of patients experiencing regrowth 2−3 cm from the initial tumor.[2,5] Treatment of GBM results in neurodegenerative side effects for most patients due to the cytotoxicity of radiation and chemotherapy agents.[2,5,9] These side effects include mood disorders, pulmonary fibrosis, and difficulty with learning, memory, executive function, and attention.[2,5,9] Further, many patients experience little or no benefit from this painful treatment regimen due to damaged tumor cells undergoing effective DNA repair or cells acquiring mutations that inactivate transcription factor p53, which triggers apoptosis following DNA damage.[6] Additionally, cross-talk between apoptosis, autophagy, and DNA repair has been shown to lead to treatment resistance in GBM cells.[10] This motivates the development of a treatment that activates apoptosis via a transcription-independent pathway.[6]

Tumor necrosis factor-related apoptosis-inducing ligand (TRAIL), a member of the tumor necrosis factor alpha family, induces apoptosis in cancer cells via death receptor activation, a transcription-independent mechanism.[6,11,12] This ligand is expressed on the surface of activated natural killer (NK) cells, macrophages, dendritic cells (DCs), and T cells as it serves a role in the innate immune response.[13−15] TRAIL has been found to trigger apoptosis in a number of tumor cell types by binding to death receptors 4 and 5 (DR4/5).[12,13,16] This association leads to receptor trimerization, followed by the intracellular binding of

Received: February 13, 2023
Accepted: April 19, 2023
Published: May 3, 2023

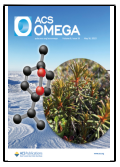

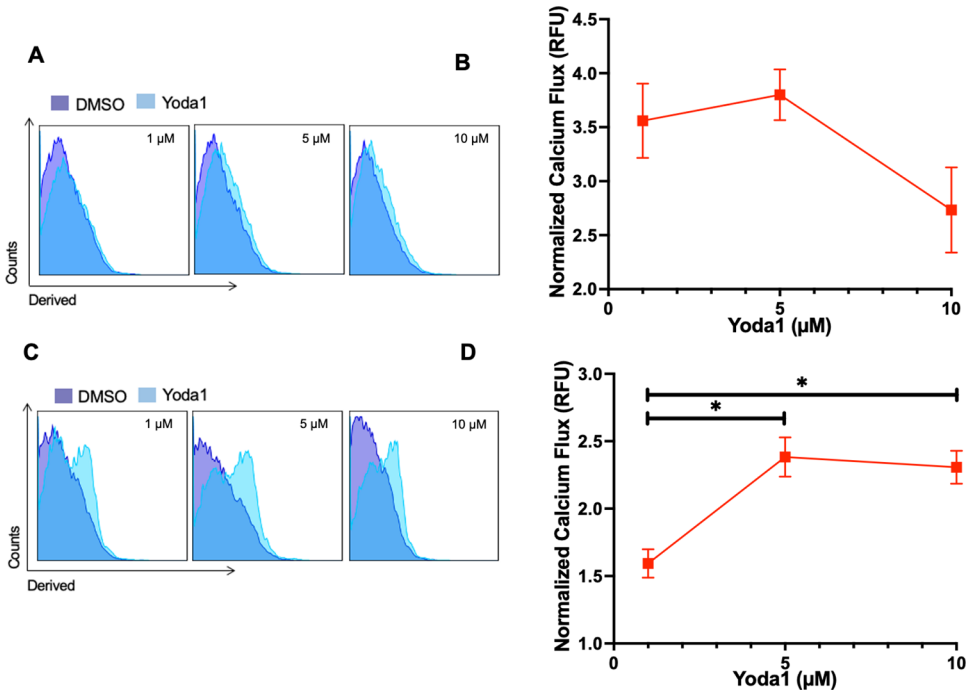

Figure 1. Ca^{2+} flux analysis in U87 and LN18 cells treated with Yoda1. (A, C) Comparison of Ca^{2+} influx in U87 (A) and LN18 (C) cells treated with different concentrations of Yoda1. DMSO was used as a vehicle control. (B, D) Yoda1-induced Ca^{2+} influx in RFU normalized to DMSO control for each treatment concentration in U87 (B) and LN18 (D) cells. *$p < 0.05$.

Fas-associated death domains (FADD) and caspase-8, which forms the death-inducing signaling complex (DISC).[12,13,16] TRAIL is of particular interest for cancer therapy because of its ability to induce apoptosis in tumor cells without harming normal cells.[12,17] This selectivity is due, in part, to the abundance of decoy receptors in healthy tissues.[17]

In a previous study, mice treated with E-selectin (ES)-TRAIL liposomes experienced a 94% decrease in prostate cancer circulating tumor cells (CTCs) and demonstrated the potential of TRAIL to prevent primary tumor metastasis.[18] However, xenografted animal studies also showed that TRAIL alone is rarely successful against the primary tumor itself.[19] Moreover, approximately 50% of tested tumor cell lines exhibit some level of TRAIL resistance, and GBM is particularly resistant to TRAIL.[6,11] Therefore, for TRAIL to become a viable therapy, cancer cells must become sensitized to TRAIL. One way in which TRAIL can become sensitized is through the fluid shear stress (FSS) that CTCs experience in the circulation.[12] Alternatively, under static conditions, TRAIL resistance can be overcome with molecular therapeutics using molecules such as aspirin, taxanes, and piperlongumine.[20−23] Previous studies have found that the activation of the mechanosensitive ion channel Piezo1 via the agonist Yoda1 also induces TRAIL sensitization under static conditions and have characterized the toxicity of this treatment using HUVEC cells as a non-cancerous control.[12,24] The mechanism by which the small-molecule Yoda1 activates Piezo1, a mechanosensitive Ca^{2+} ion channel, is currently unknown.[24−26] However, Ca^{2+} influx through Piezo1 is known to lead to a number of cellular responses, including apoptosis.[27] In vivo, Yoda1 was found to cause a significant increase in apoptosis in prostate cancer, breast cancer, and colon cancer cell lines compared to TRAIL alone.[12]

The current study examines for the first time the effects of Piezo1 activation on TRAIL-mediated apoptosis in glioblastoma cells. Specifically, we aimed to characterize the Yoda1 + TRAIL cell death pathway and the efficacy of a Yoda1 + TRAIL treatment compared to appropriate control conditions and the standard chemotherapy treatment TMZ.[28] Piezo1 was also activated via FSS to further explore the relationship between Piezo1 activation and TRAIL-mediated apoptosis in GBM cells since FSS has been shown to sensitize colon and prostate cancer cells to TRAIL.[12,29] The therapeutics in this study were tested in immortalized U87 MG (U87) cells, which are TMZ-sensitive and exhibit an invasive phenotype, and LN18 cells which are TMZ-resistant and less invasive.[28,30]

RESULTS

Yoda1 Treatment Increases Ca^{2+} Influx in GBM Cells.

Piezo1 is a mechanosensitive Ca^{2+} ion channel found on the plasma membrane. Ca^{2+} influx through Piezo1 in GBM cells was quantified with a Ca^{2+} flux assay to determine the extent to which Yoda1 can activate Piezo1 under static conditions. Fluo-4 and Fura Red are both fluorescent dyes that bind to intracellular Ca^{2+} and therefore allow for the quantification of Ca^{2+} influx.[31] GBM cells were treated with 1, 5, and 10 μM treatments of dimethyl sulfoxide (DMSO) and Yoda1, with DMSO serving as a vehicle control. Ca^{2+} influx was measured immediately after treatment.

For both the U87 and LN18 cells, there was a significant increase in Ca^{2+} influx for the Yoda1 treatment at every concentration relative to the DMSO control. When normalized to the DMSO control, there was not a significant difference between the Ca^{2+} influx, measured in ratiometric flux units (RFU), for varied Yoda1 concentrations in U87 cells. However, there was a significant increase in the Ca^{2+} influx of LN18 cells with the 5 and 10 μM Yoda1 treatments, compared to the 1 μM treatment. These results indicate that Piezo1 on U87 cells becomes saturated at lower Yoda1 concentrations than Piezo1 on LN18 cells (Figure 1A−D).

https://doi.org/10.1021/acsomega.3c00705
ACS Omega 2023, 8, 16975−16986

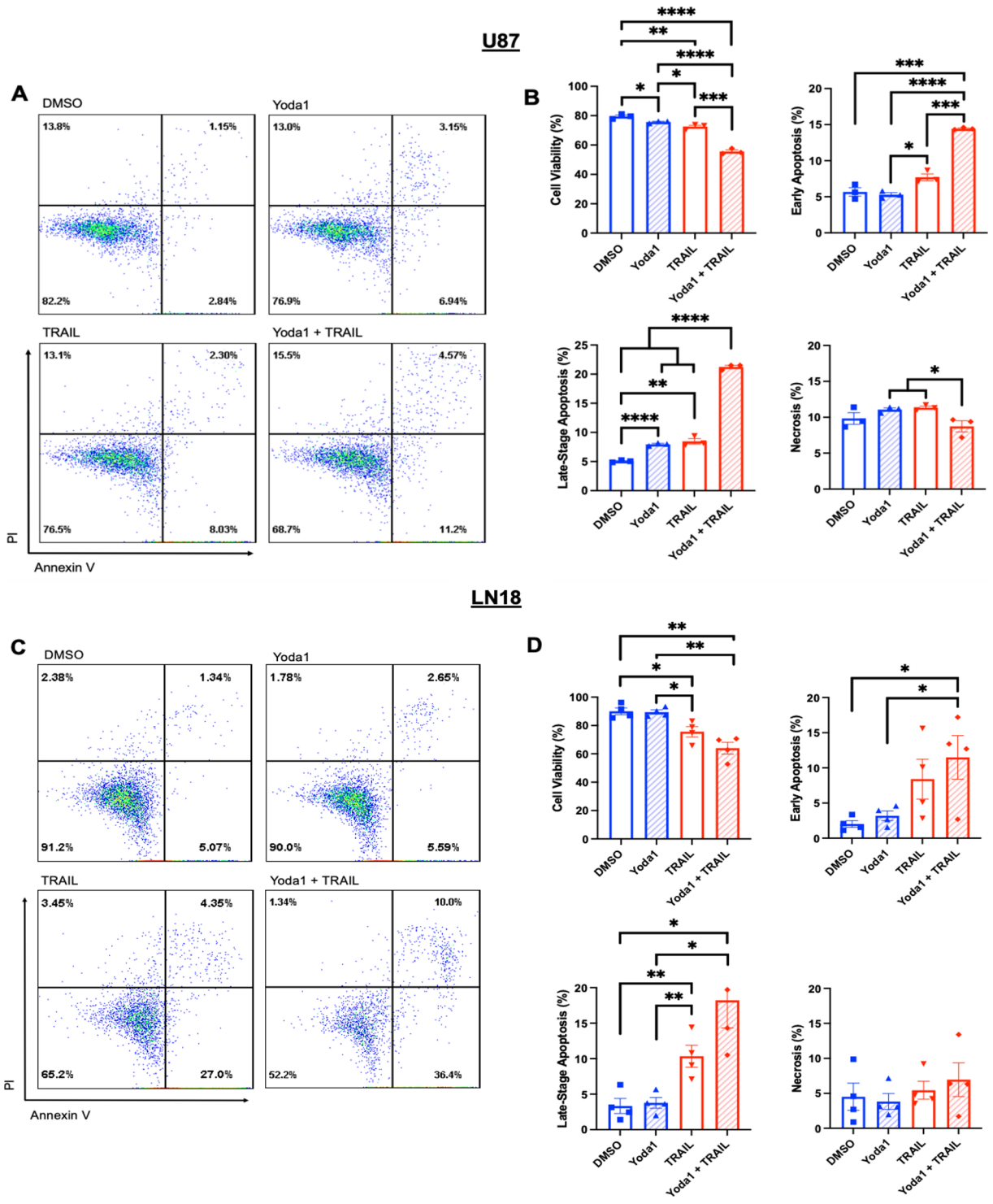

Figure 2. Cell viability analysis following Yoda1 + TRAIL treatment. (A, C) Representative flow cytometry plots of AV-PI data for DMSO, Yoda1, TRAIL, and TRAIL + Yoda1 treatments of U87 cells (A) and LN18 cells (C). (B, D) Comparison of viable, early apoptotic, late apoptotic, and necrotic cells 24 h after each U87 treatment (B) and 4 h after each LN18 treatment (D). *$p < 0.05$, **$p < 0.01$, ***$p < 0.005$, ****$p < 0.001$.

Cell Viability Decreases in GBM Cells Following Combined Yoda1 and TRAIL Treatment. An Annexin V-propidium iodide (AV-PI) viability assay was used to measure cell viability, apoptosis, and necrosis in GBM cells following Yoda1 + TRAIL treatment. Representative flow cytometry plots showed an overall decrease in cell viability and an increase in late-stage apoptosis for U87 cells treated with 10 μM Yoda1 + 25 ng/mL TRAIL compared to control conditions (Figure 2A). Dose response curves were generated for U87 cells to determine the optimal Yoda1 and TRAIL concentrations for treatments (Figure S1A, B). 24 h after treatment, U87 cells treated with Yoda1 + TRAIL showed a significantly lower mean cell viability of 56 ± 1.1% compared to the DMSO control which had a mean viability of 80 ± 0.93% (Figure 2B). A significantly greater portion of cells treated with Yoda1 + TRAIL was found to be in early-stage apoptosis (14 ± 0.09%) when compared to the

https://doi.org/10.1021/acsomega.3c00705
ACS Omega 2023, 8, 16975−16986

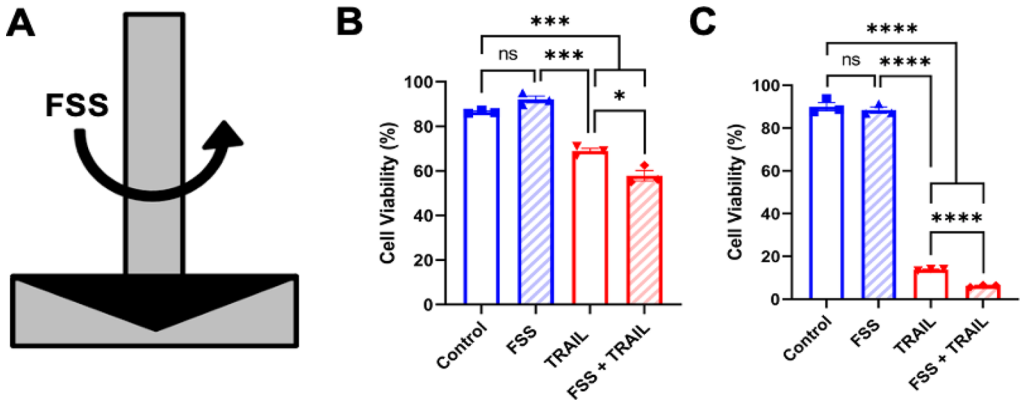

Figure 3. Cell viability analysis for combination FSS + TRAIL treatment. (A) Schematic of the cone and plate viscometer. (B) Cell viability following FSS and/or TRAIL treatment in U87 cells. (C) Cell viability following FSS and/or TRAIL treatment in LN18 cells. No significance (ns), *$p < 0.05$, ***$p < 0.005$, ****$p < 0.001$.

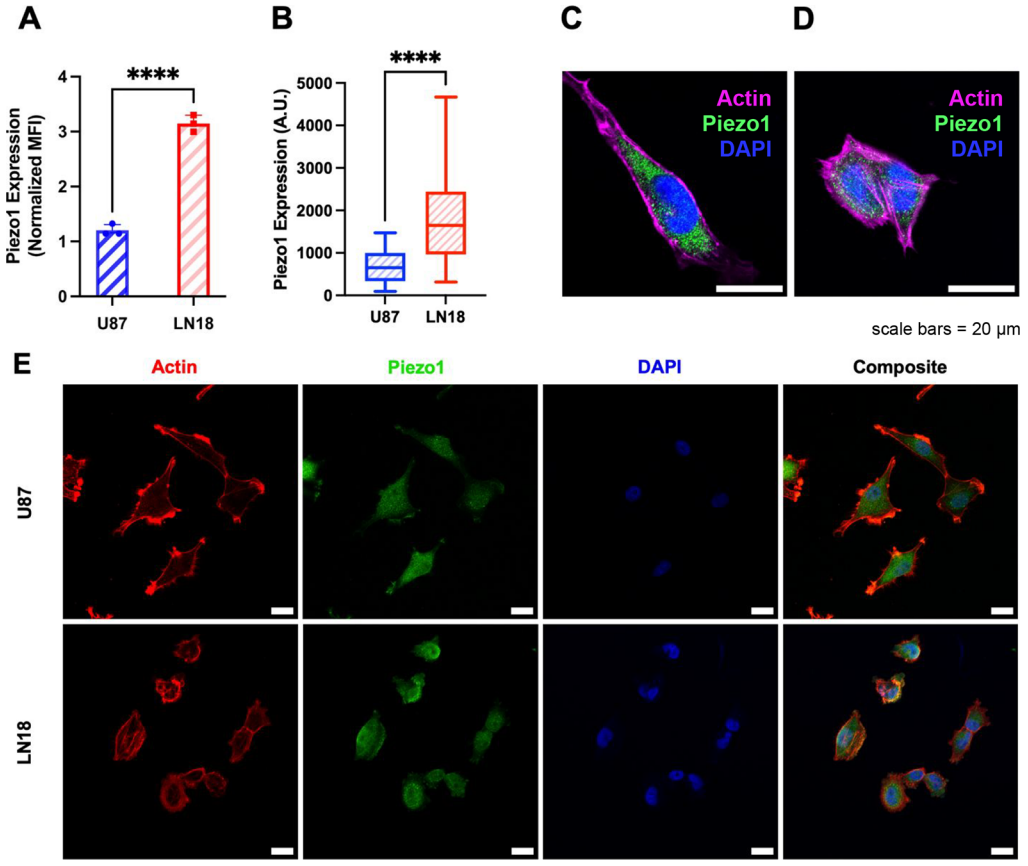

Figure 4. Analysis of Piezo1 expression. (A) Comparison of flow cytometry data quantifying Piezo1 expression in U87 and LN18 cells. (B) Confocal image data comparing the expression of Piezo1 on GBM cells. Representative high magnification images of U87 cells (C) and LN18 cells (D). (E) Composite and representative lower magnification images of actin, Piezo1, and DAPI staining (respectively) in GBM cells. *$p < 0.05$, **$p < 0.01$, ***$p < 0.005$, ****$p < 0.001$. Scale bar = 20 μm.

DMSO vehicle control (5.7 ± 0.58%) (Figure 2B). An increase in late-stage apoptosis was seen with the Yoda1 + TRAIL treatment compared to the DMSO control with the mean percentage of cells in late-stage apoptosis being 21 ± 0.27 and 5.1 ± 0.10%, respectively (Figure 2B). There was a significant difference between necrotic cells in some treatment groups, but this difference was minimal (Figure 2B).

LN18 cells treated with 10 μM Yoda1 + 25 ng/mL TRAIL also showed a decrease in viability and an increase in early and late-stage apoptosis compared to control conditions (Figure 2C). At 24 h post-treatment, the cell death was too great to quantify, so the time point was shortened to 4 h for this cell line. The mean cell viability for cells 4 h after treatment with Yoda1 + TRAIL was 64 ± 4.1%, compared to the DMSO control which had a mean cell viability of 90 ± 2.4% (Figure 2D). For the Yoda1 + TRAIL treatment, 12 ± 3.1% of the cells were determined to be in early-stage apoptosis compared to the DMSO control (2.0 ± 0.49%) (Figure 2D). The mean percentage of cells in late-stage apoptosis for the Yoda1 + TRAIL treatment was 18 ± 3.9% compared to the DMSO

https://doi.org/10.1021/acsomega.3c00705
ACS Omega 2023, 8, 16975−16986

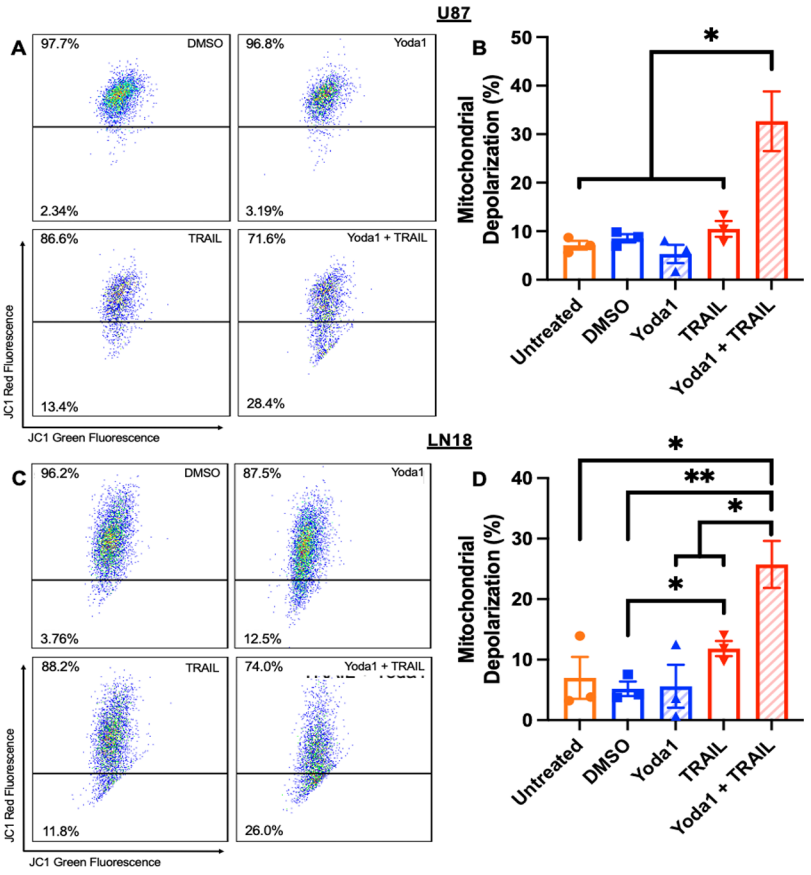

Figure 5. Mitochondrial depolarization analyzed after Yoda1 + TRAIL treatment. (A,C) Representative flow cytometry plots of JC-1 assay for DMSO, Yoda1, TRAIL, and Yoda1 + TRAIL treatments of U87 cells (A) and LN18 cells (C). (B,D) Comparison of mitochondrial depolarization 24 h after each U87 cell treatment (B) and 4 h after each LN18 cell treatment (D). *$p < 0.05$, **$p < 0.01$.

control which had 3.3 ± 1.1% of cells in late-stage apoptosis (Figure 2D). The necrotic LN18 cells showed no significant difference between any of the treatment groups (Figure 2D).

Cell Viability Decreases in GBM Cells Following FSS-Induced Mechanical Activation of Piezo1 and TRAIL Treatment. FSS applied via a cone-and-plate viscometer (Figure 3A) can be used to mechanically activate Piezo1.[12] This experiment was performed to confirm the results produced when Piezo1 was activated via Yoda1 since Piezo1 is a mechanosensitive ion channel. Cone-and-plate viscometers were used to apply 5.0 dyn/cm^2 of FSS to GBM cells for 1 h with and without the presence of TRAIL to further explore the effects of Piezo1 activation on TRAIL sensitization. The FSS + TRAIL combination treatment resulted in a significant decrease in cell viability in U87 (57.9 ± 2.34%) and LN18 (6.26% ± 0.30%) cells when compared to the TRAIL-treated U87 (68.9% ± 1.18%) and LN18 (13.77% ± 0.23%) cells in the absence of FSS (Figure 3B,C). These findings further demonstrate the efficacy of enhancing TRAIL-mediated apoptosis via Piezo1 activation.

LN18 Cells Exhibit Greater Piezo1 Expression Than U87 Cells. Since LN18 cells were found to be significantly more sensitized to TRAIL by chemical and mechanical activation of Piezo1 compared to the U87 cells, the relative Piezo1 expression on the cells was examined to see if a difference in Piezo1 expression could account for the observed responses. The cells were stained with an extracellular Piezo1 antibody, and the normalized median fluorescence intensity (MFI) was measured using a flow cytometer to determine that LN18 cells expressed significantly more Piezo1 than U87 cells, with LN18 and U87 cells exhibiting mean Piezo1 expression levels of 3.1 ± 0.087 and 1.2 ± 0.060, respectively (Figure 4A). These results were further corroborated by analysis of confocal images of GBM cells stained for Piezo1 (Figure 4B−E). Specifically, LN18 cells were found to express more than 2.5× the amount of Piezo1 found in U87 cells. The cells exhibited mean Piezo1 expression levels of 1780 ± 122 and 690.2 ± 44.50 A.U., respectively (Figure 4B). Actin expression was also explored at this time using confocal imaging (Figure S2).

Combined Treatments with Yoda1 and TRAIL Increase Mitochondrial Depolarization in GBM Cells. Piezo1 has been shown to sensitize PC3 prostate cancer cells to TRAIL through the intrinsic apoptosis pathway, where Ca^{2+} influx through Piezo1 activates calpains and subsequently amplifies the death-inducing signals in the TRAIL-mediated apoptosis pathway (Figure 7).[12] These proapoptotic proteases induce the formation of pores in the mitocondrial membrane, which leads to mitochondrial outer membrane permeability (MOMP).[12] MOMP is the key event in the intrinsic apoptosis pathway and is mediated by the Bcl-2 family proteins, such as Bax and Bak.[32] Ultimately, MOMP results in the release of apoptotic proteins through the mitochondrial pores, leading to numerous cell death pathways.[12,32] Mitochondrial depolarization was examined to quantify the occurrence of MOMP and the intrinsic apoptotic pathway in GBM cells.

A JC-1 assay was used to quantify the mitochondrial depolarization in GBM cells. A significant increase in mitochondrial depolarization was seen in U87 cells 24 h after

https://doi.org/10.1021/acsomega.3c00705
ACS Omega 2023, 8, 16975−16986

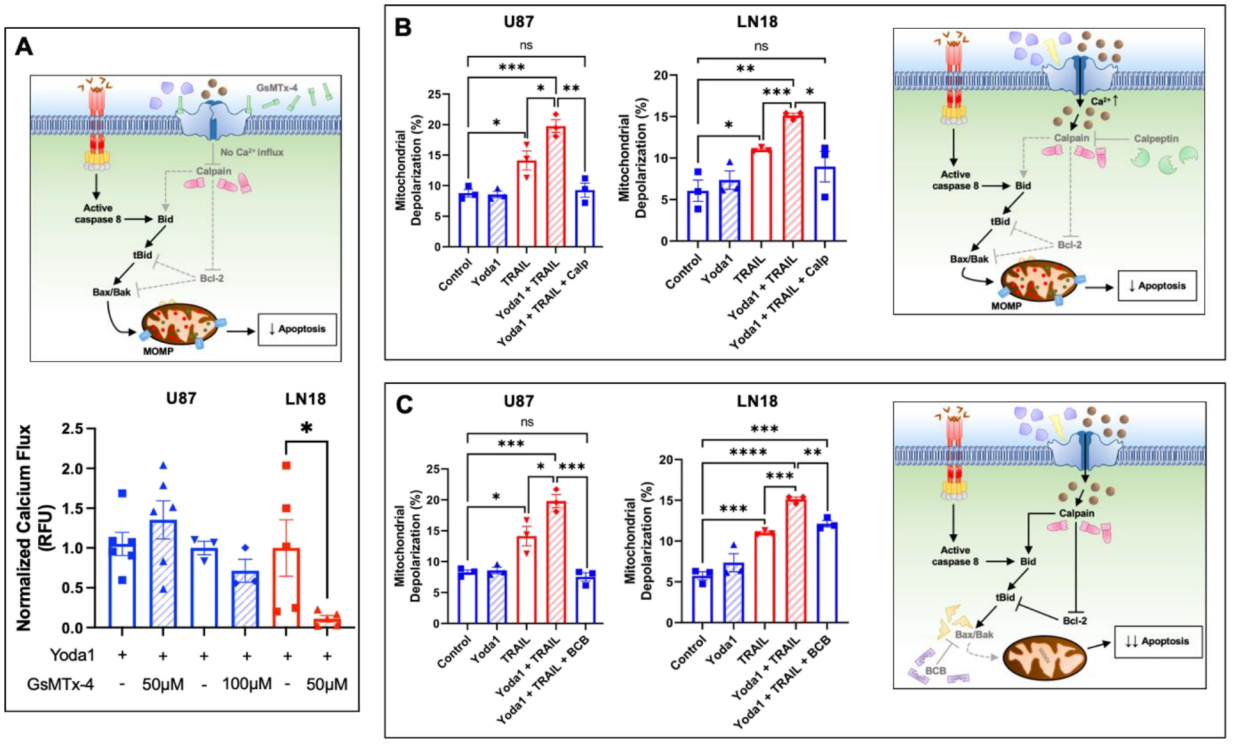

Figure 6. Cell viability after inhibition of the Yoda1 + TRAIL apoptotic pathway. (A) The effect of GsMTx-4 on Piezo1 represented by the normalized Ca^{2+} influx in GBM cells following GsMTX-4 inhibition. (B) The effect of calpeptin (Calp) on the Yoda1 + TRAIL apoptotic pathway represented via GBM mitochondrial depolarization. (C) The effect of BCB on the Yoda1 + TRAIL apoptotic pathway represented via GBM mitochondrial depolarization. No significance (ns), $*p < 0.05$, $**p < 0.01$, $***p < 0.005$, $****p < 0.001$.

Yoda1 + TRAIL treatment (33 ± 6.1%) compared to the DMSO (8.5 ± 0.84%) and Yoda1 (5.3 ± 1.9%) controls (Figure 5A,B). Similarly, LN18 cells showed a significant increase in depolarization 4 h following treatment with 26 ± 3.9% depolarization for the Yoda1 + TRAIL treatment relative to 5.2 ± 1.2 and 5.6 ± 3.6% depolarization for the DMSO and Yoda1 controls, respectively (Figure 5C,D).

GsMTx-4 Significantly Inhibits Piezo1 in LN18 Cells. GsMTx-4 is a mechanosensitive ion channel inhibitor that blocks Ca^{2+} influx through a family of ion channels that includes Piezo1.[33] The Ca^{2+} flux assay was repeated on GBM cells, with cells treated with either 50 μM Hank's balanced salt solution (HBSS) buffer containing Ca^{2+} or 50 μM of the inhibitor prior to staining and 5 μM Yoda1 and 5 μM DMSO treatments. GsMTx-4 treatment of U87 cells at low concentrations did not consistently reduce Ca^{2+} influx but was able to successfully reduce Ca^{2+} influx in all LN18 replicates, leading to decreased Ca^{2+} influx relative to the control (Figure 6A). These results reflected the lower levels of Piezo1 expression in U87 cells. When U87 cells were treated with a greater concentration of GsMTx-4 (100 μM), a trend of increased inhibition leading to decreased Ca^{2+} influx was observed (Figure 6A).

Calpain and Bax Inhibition Decreases Mitochondrial Depolarization Following Yoda1 and TRAIL Treatment in GBM Cells. Calpeptin is an inhibitor of calpain, an essential component of the Piezo1 pathway.[12] JC-1 mitochondrial depolarization assays were repeated on GBM cells with inhibitor treatment prior to TRAIL, Yoda1, and vehicle control treatments. Calpain inhibition resulted in a significant decrease in mitochondrial depolarization with treatment of Yoda1 + TRAIL in U87 (9.27% ± 1.16%) and LN18 (8.97% ± 1.85%) cells compared to the Yoda1 + TRAIL-treated U87 (19.76% ± 1.05%) and LN18 (15.13% ± 0.27%) groups in the absence of calpeptin (Figure 6B). Interestingly, no significance was observed between the control and inhibitor-treated groups for both GBM cell lines.

Bax channel blocker (BCB) is an inhibitor of Bax, a component of the intrinsic apoptosis pathway that triggers MOMP.[12] The JC-1 mitochondrial depolarization assays were repeated on GBM cells with inhibitor treatment prior to TRAIL and vehicle control treatments. Bax inhibition resulted in a significant decrease in mitochondrial depolarization following the treatment of Yoda1 + TRAIL in U87 (7.53% ± 0.69%) and LN18 (12.1% ± 0.39%) cells compared to the Yoda1 + TRAIL-treated U87 (19.8% ± 1.04%) and LN18 (15.13% ± 0.27%) groups in the absence of BCB (Figure 6C).

Characterization of Mechanism: Yoda1 Synergistically Enhances the TRAIL Apoptotic Pathway through Piezo1 Activation. Our previous studies have demonstrated that Piezo1 sensitizes PC3 prostate cancer cells to TRAIL through the intrinsic apoptosis pathway.[12] The observed mitochondrial depolarization in U87 and LN18 cells following Yoda1 + TRAIL treatment indicates the involvement of this pathway in GBM cells (Figure 7). Reduction in cell death following inhibition of Calpain and Bax, proapoptotic proteins in this pathway, further supports this finding. This pathway, previously explored in Hope et al.,[12] is illustrated below in addition to the effect of inhibitors used in this GBM study (GsMTx-4, Calpeptin, and BCB) on the pathway.

Clinical Implications: Yoda1 + TRAIL Results in Higher Rates of Apoptosis in LN18 Cells In Vitro Compared to the Current Standard of Care. TMZ is the standard chemotherapy used to treat GBM.[28] U87 cells have been shown to be sensitive to TMZ, while LN18 cells are known to be

https://doi.org/10.1021/acsomega.3c00705
ACS Omega 2023, 8, 16975−16986

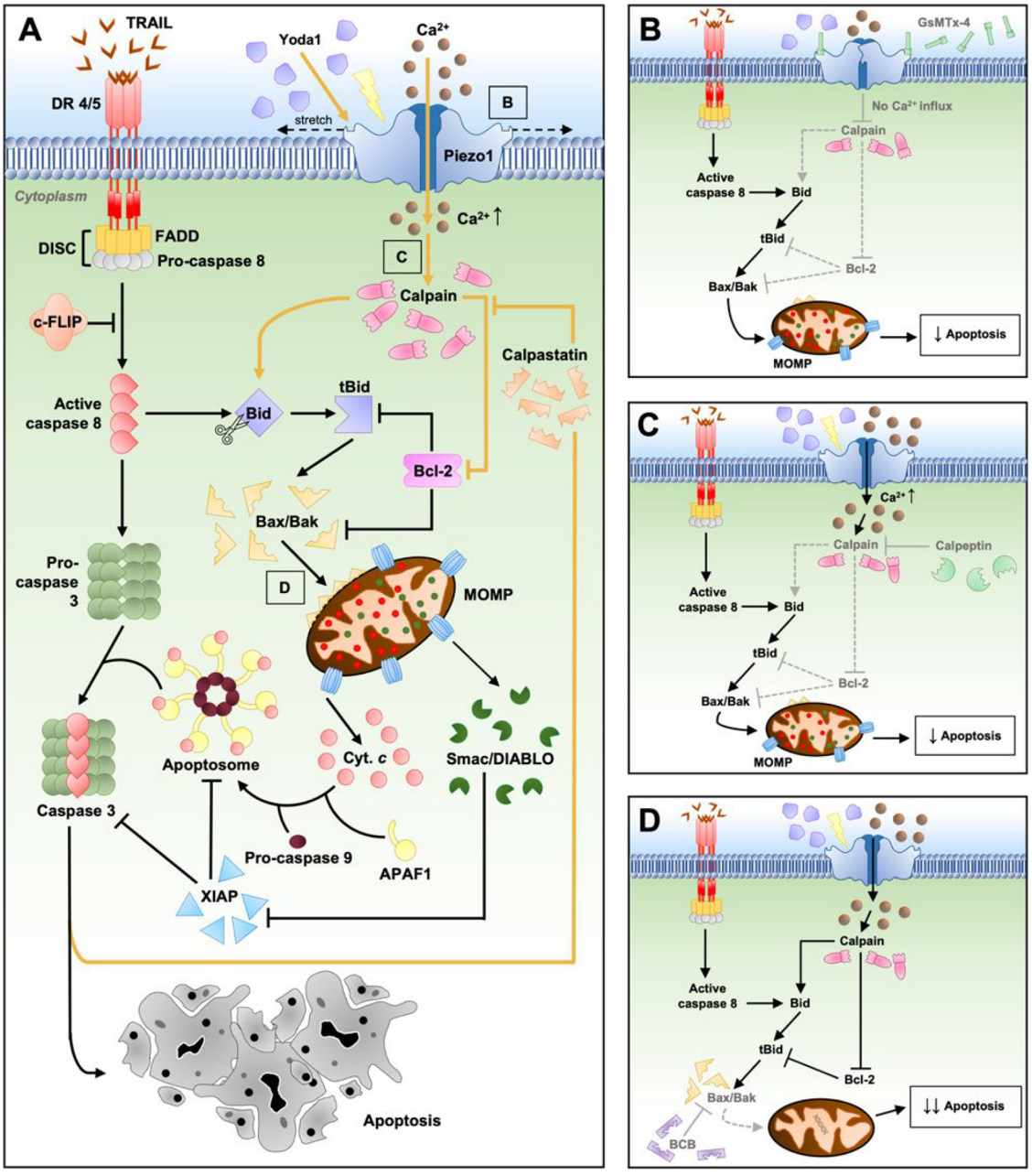

Figure 7. Yoda1 + TRAIL apoptotic pathway. (A) Yoda1 is able to activate Piezo1, a mechanosensitive ion channel, under static conditions. This leads to Ca^{2+} influx and a signaling cascade that enhances TRAIL-induced permeabilization of the mitochondria, resulting in increased apoptosis. (B) GsMTx-4 inhibits Piezo1 and other mechanosensitive ion channels, decreasing Ca^{2+} influx and the synergistic effects of Yoda1. (C) Calpeptin inhibits calpain, decreasing the effect of extracellular Ca^{2+} and leading to increased cell viability following treatment. (D) Bax channel blocker (BCB) inhibits Bax, blocking the effects of both Yoda1 and TRAIL, largely increasing cell viability.

resistant to the drug.[28] AV-PI assays were performed to determine the in vitro efficacy of the Yoda1 + TRAIL treatment compared to the current standard of care.

U87 cells were found to exhibit similar levels of sensitivity to the Yoda1 + TRAIL (10 and 25 ng/mL) treatment and low- and high-dose TMZ treatments (50, 200 μM) (Figure 8A). 24 h following treatment, the respective mean cell viabilities for Yoda1 + TRAIL, low-dose TMZ, and high-dose TMZ were 78.4 ± 2.23, 69.4 ± 2.43, and 72.0 ± 2.02% (Figure 8C). At 72 h, there was less difference between the effects of the treatments with mean cell viabilities of 74.3 ± 1.28, 71.4 ± 2.90, and 77.5 ± 3.08% for the Yoda1 + TRAIL, low-dose TMZ, and high-dose TMZ treatments (Figure 8D).

The LN18 cells, which are known to be resistant to TMZ, were significantly more sensitive to the Yoda1 + TRAIL treatment (Figure 8B). 4 h post-treatment, the cell viability for the Yoda1 + TRAIL treatment (45.9 ± 4.49%) was found to be significantly lower than the cell viability for both the low-dose (68.8 ± 2.98%) and high-dose (63.5 ± 1.98%) TMZ treatments (Figure 8E). After 8 h, the cell viability for the Yoda1 + TRAIL treatment decreased (40.7 ± 4.86%), while the cell viability for the low-dose (76.5 ± 5.03%) and high-dose (75.1 ± 5.24%) TMZ treatments increased (Figure 8F). Therefore, an even greater difference in the efficacy of these two treatments was observed over an 8 h period.

https://doi.org/10.1021/acsomega.3c00705
ACS Omega 2023, 8, 16975−16986

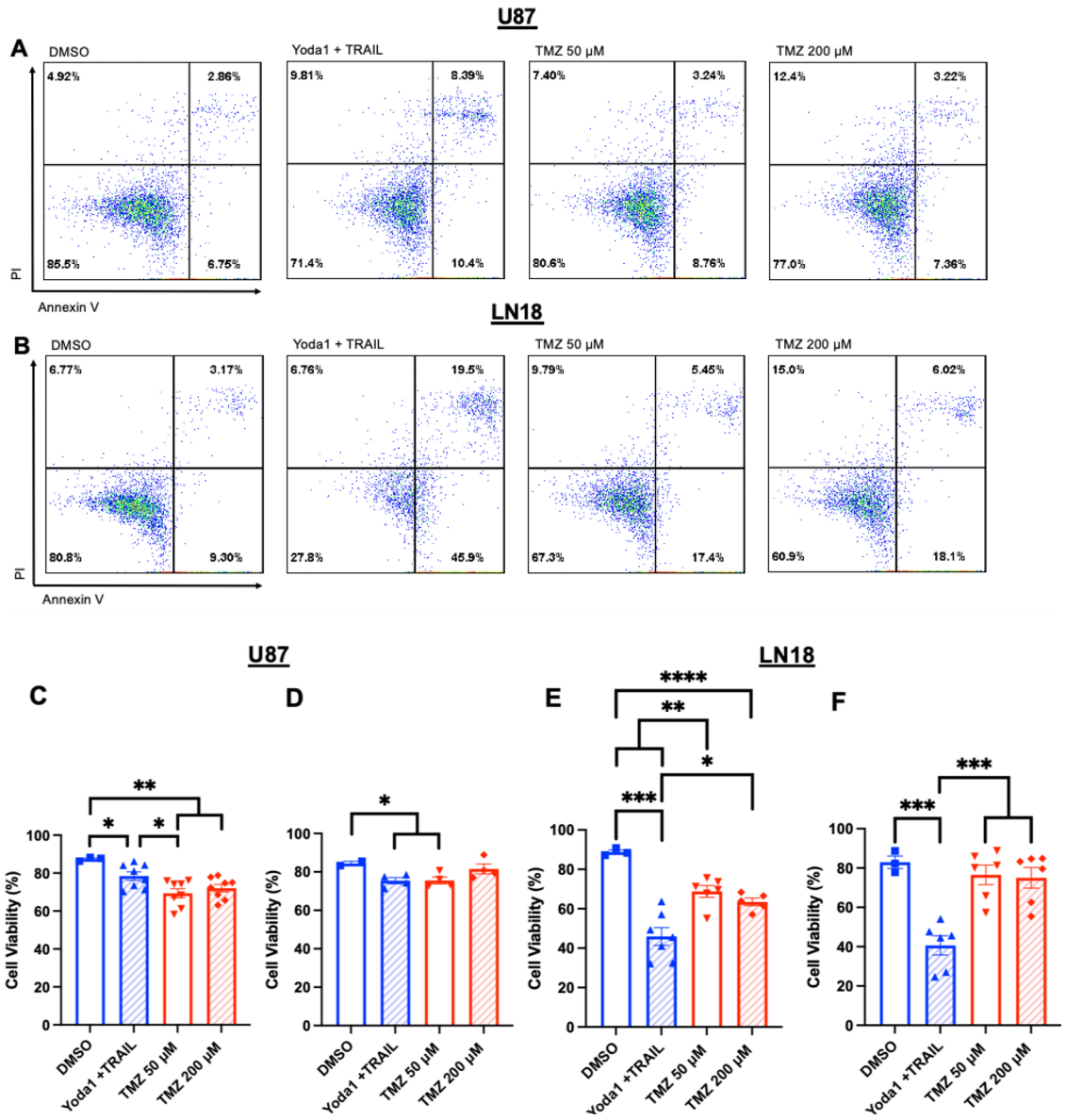

Figure 8. Comparison of cell viabilities following Yoda1 + TRAIL and TMZ treatments. (A, B) Representative flow plots of AV-PI data for DMSO, Yoda1, TRAIL, and Yoda1 + TRAIL treatments of U87 cells after 72 h (A) and LN18 cells after 8 h (B). (C, D) Comparison of viable, early apoptotic, late apoptotic, and necrotic cells for U87 treatments after 24 (C) and 72 h (D). (E, F) Comparison of LN18 cells 4 (E) and 8 h (F) after treatment. *p < 0.05, **p < 0.01, ***p < 0.005, ****p < 0.001.

DISCUSSION

Previous studies have shown that Piezo1 activation can enhance the apoptotic effect of TRAIL, an immune chemical that can selectively target cancer cells. Compared to most cell lines, GBM cells are particularly resistant to TRAIL, and this study aimed to characterize the effect of Piezo1 activation on TRAIL sensitization in GBM cells.

Exploring Ca^{2+} influx and cell viability following the chemical and mechanical activation of Piezo1 provided insight into the effect of this ion channel on the TRAIL-mediated apoptosis pathway. In both GBM cell lines, Ca^{2+} influx significantly increased with Yoda1 treatment relative to a vehicle control. These results indicated that Yoda1 effectively activates Piezo1, a mechanosensitive Ca^{2+} ion channel, under static conditions. Additionally, the results suggested that Piezo1 becomes saturated on U87 cells at lower concentrations of Yoda1 compared to LN18 cells, which is likely because U87 cells were shown to exhibit significantly lower levels of Piezo1 expression relative to LN18 cells in both flow cytometry and confocal microscopy. These results also explain why GsMTx-4 was able to successfully reduce Ca^{2+} influx in LN18 cells at lower concentrations than in U87 cells. This induced Ca^{2+} influx may have implications related to the regulation of tumorigenesis in GBM cells. Ca^{2+} is a ubiquitous secondary messenger that can cause a host of cellular responses in cancer cells including the regulation of this process.[27] Although this relationship is not well studied in glioblastoma, this mechanism has been established in breast and ovarian cancer.[34,35]

Yoda1 + TRAIL treatments resulted in a significant decrease in cell viability and increase in apoptosis relative to controls 24 h after treatment of the U87 cells and 4 h after treatment of the LN18 cells. This finding demonstrates that the chemical activation of Piezo1 under static conditions enhances TRAIL-mediated apoptosis through Ca^{2+} influx. Similar findings with

https://doi.org/10.1021/acsomega.3c00705
ACS Omega 2023, 8, 16975−16986

the FSS + TRAIL treatment further support that Piezo1 activation, via chemical or mechanical activation, is directly responsible for the enhanced TRAIL sensitization observed in GBM cells. In the future, different shear rates could be assessed to determine the optimal force for Piezo1 activation in GBM cells.

Initially, the cell viability assays were conducted 24 h after Yoda1 + TRAIL treatment for both cell lines. However, LN18 cell death was found to be too extensive to quantify at this time point, so the experimental timeframe was shortened to 4 h. The difference in Yoda1 + TRAIL sensitivity between the cell lines is likely due to the higher expression of Piezo1 on LN18 cells compared to that on the U87 cells. Higher Piezo1 expression in LN18 cells allows for increased Ca^{2+} influx, which explains why LN18 cells were more significantly sensitized to TRAIL by Yoda1 treatments compared to the U87 cells.

Mitochondrial depolarization assays were performed to further characterize the mechanism in which Piezo1 activation enhances TRAIL sensitization as increased mitochondrial depolarization indicates the execution of intrinsic apoptosis. Inhibition of Calpain and Bax, two key proapoptotic proteases in the Yoda1 + TRAIL apoptotic pathway, resulted in significantly lower levels of apoptosis in both GBM cell lines. These findings suggest that GBM cells execute the same Yoda1 + TRAIL apoptotic pathway previously outlined in prostate cancer cell lines, which relies heavily on intrinsic apoptosis.[12] This pathway is a transcription-independent mechanism that is known to target cancer cells, leaving healthy cells relatively unharmed.[17] Therefore, the observed apoptosis speaks to the potential viability of Yoda1 + TRAIL as a cancer therapeutic.

Previous studies have shown that LN18 cells are more resistant to TMZ than U87 cells.[36] TMZ is a chemotherapy commonly prescribed with radiotherapy as the first line of defense against GBM since it is one of a few cancer drugs that can penetrate the blood−brain barrier.[37] TMZ has toxic side effects and is not a transcription-independent method of targeting cancer cells, so GBM cells can become resistant to the therapy, resulting in tumor reoccurrence.[37] The LN18 cells were found to be more responsive to the Yoda1 + TRAIL treatment than high and low dose TMZ treatments since Yoda1 + TRAIL utilizes a different, transcription-independent pathway. U87 cells, with lower expression levels of Piezo1, responded comparably to both treatments. The sensitivity of these GBM cells to the Yoda1 + TRAIL treatment suggests that this therapy may be successful in targeting tumors that are particularly resistant to the current standard treatment. Therefore, the efficacy of the Yoda1 + TRAIL treatment compared to TMZ in vitro demonstrates promise for this combination therapy as a potential GBM therapeutic. However, extensive research into the effects on this treatment in vivo and the toxicity, biodistribution, and pharmacokinetics needs to be further explored before the potential of this therapeutic can be fully understood.

CONCLUSIONS

Chemical and mechanical activation of Piezo1 via FSS and Yoda1 has been shown to increase TRAIL-mediated cell death in both U87 and LN18 cell lines. LN18 cells were found to have higher levels of Piezo1 expression and increased sensitivity to these combination treatments compared to U87 cells. Further, this pathway was characterized through inhibition experiments that revealed it heavily involves internal apoptosis. The pathway is transcription independent, and therefore, LN18 cells, which are resistant to the standard chemotherapy TMZ, were significantly more sensitive to the Yoda1 + TRAIL combination therapy than the current standard of care in vitro.

MATERIALS AND METHODS

Reagents and Antibodies. Eagle's minimum essential medium (EMEM) cell culture media containing non-essential amino acids, 2 mM L-glutamine, 1 mM sodium pyruvate, and 1500 mg/L sodium bicarbonate were obtained from Gibco (Grand Island, NY, USA), as was Dulbecco's modified Eagle's medium (DMEM) cell culture media containing 4 mM L-glutamine, 4500 mg/L glucose, 1 mM sodium pyruvate, and 1500 mg/L sodium. Fetal bovine serum (FBS), penicillin−streptomycin (PS), and HBSS were also purchased from Gibco. DMSO and bovine serum albumin (BSA) were obtained from Sigma-Aldrich (St. Louis, MO, USA). Yoda1, Calpeptin, and Bax channel blocker (BCB) were obtained from Tocris Bioscience (Bristol, United Kingdom). Fura Red (ratiometric) and Fluo-4 (non-ratiometric) Ca^{2+} fluorescence dyes were purchased from Invitrogen (Waltham, MA, USA). FITC-conjugated AV and PI were obtained from BD Pharmingen (San Diego, CA, USA). JC-1 mitochondrial membrane dye and GsMTx-4 were obtained from Abcam (Waltham, MA, USA). TRAIL was obtained from PeproTech (Cranbury, NJ, USA). Polyclonal Rabbit Piezo1 Antibody [Alexa Fluor 488] and Rabbit IgG Isotype Control [Alexa Fluor 488] were obtained from Novus Biologicals (Centennial, CO, USA). Unconjugated Piezo1 polyclonal antibody was purchased from Proteintech (Rosemont, IL, USA). 32% Paraformaldehyde aqueous solution (electron microscopy grade) was purchased from Electron Microscopy Sciences (Hatfield, PA, USA). VECTASHIELD Antifade Mounting Medium was obtained from Vector Laboratories (Newark, CA, USA). Tween 20, viscous liquid, CAS 9005-64-5 (P1379), poly-L-lysine solution, Triton X-100, and DAPI (D9542-10MG) (Sigma-Aldrich) and ActinRed 555 ReadyProbes Reagent and secondary antibody Alexa Fluor 488 goat anti-rabbit IgG (H + L) (Invitrogen) were purchased for confocal imaging. 10% Normal Goat Serum was also purchased for confocal imaging from Life Technologies (Carlsbad, CA, USA). TMZ was obtained from Sigma-Aldrich.

Cell Culture. U87 cells were cultured in EMEM cell culture media supplemented with 10% FBS and 1% penicillin-streptomycin. LN18 cells were cultured in DMEM cell culture media supplemented with 5% FBS and 1% PS. Both U87 and LN18 cell lines were incubated under humidified conditions (37 °C and 5% CO_2), and experiments were performed at ∼80% confluency.

Ca^{2+} Flux Assay. The GBM cells were lifted and resuspended at 5×10^5 cells per 1 mL of unsupplemented DMEM. The cells were stained with 1 μL of 1 μM Fluo-4 and 2 μL of 1 μM Fura Red and then incubated for 30 min. The cells were washed with HBSS buffer containing Ca^{2+} and incubated for 30 min at RT. Cells were concentrated to 5×10^4 cells/200 μL HBSS and treated with DMSO or Yoda1 at various concentrations (1, 5, and 10 μM). The cells were transferred to a 96-well plate, and the fluorescence of each sample was measured in a Guava easyCyte 12HT flow cytometer. The data were analyzed by dividing green-blue fluorescence (525 nm emission, 488 nm excitation) by red-blue fluorescence (696 nm emission, 488 nm excitation) and normalizing to the DMSO control.

GsMTx-4 Inhibitor Assay. For the Ca^{2+} flux experiments that used the mechanosensitive ion channel inhibitor GsMTx-4,

https://doi.org/10.1021/acsomega.3c00705
ACS Omega 2023, 8, 16975−16986

the Ca^{2+} flux protocol previously described was followed, except the lifted cells were treated with either 50 or 100 μM HBSS buffer containing Ca^{2+} or 50 or 100 μM of the inhibitor. A 2-way ANOVA was used for analysis. Six replicates were performed on the U87 cells at the 50 μM concentration, and five replicates were performed on the LN18 cells at this concentration.

AV-PI Assay. GBM cells were plated in a 24-well plate at 5×10^4 cells per well. After 24 h, corresponding wells were treated with 10 μM DMSO, 10 μM Yoda1, 25 ng/mL TRAIL, 50 μM TMZ, and 200 μM TMZ. 4 h after LN18 treatments and 24 h after U87 treatments, the cell culture media was transferred from each well to a 1.5 mL microcentrifuge tube to collect the dead cells from each treatment, and adhered cells were lifted and combined into corresponding tubes. LN18 cells exhibited extensive cell death accompanied by cell disintegration after 24 h, so this time point was not included. Each treatment was washed with 1 mL of HBSS buffer containing Ca^{2+}. A stock solution of 3% AV, 5% PI, and 92% HBSS was prepared for staining. The cells were stained with 100 μL of the stock solution and incubated in the dark for 15 min. 100 μL of HBSS buffer was added to each of the cell suspensions, and the flow cytometer was set to detect red-blue and green-blue fluorescence. The U87 and LN18 data was analyzed using unpaired t-tests. Four replicates were completed for the LN18 experiments. A TRAIL concentration series was performed on U87 cells using an AV-PI assay to determine the optimal dosage (Figure S1A). Multiple Yoda1 concentration series were performed on U87 cells to determine the optimal dosage (Figure S1B, C). The powdered TMZ purchased from Sigma-Aldrich was dissolved in anhydrous DMSO at 25 mg/mL using a glove box at the Vanderbilt Institute for Nanoscale Science and Engineering (VINSE) analytical laboratory. The lower and higher dose experimental concentrations were selected based on previous studies conducted by Soni et al.[38]

AV binds to phosphatidylserine, a phospholipid that is exposed on the outer leaflet of the plasma membrane during apoptosis, making AV an effective indicator of cell apoptosis. PI dye is able to penetrate damaged cellular membranes and bind DNA within a cell and is therefore used to detect late apoptotic or necrotic cells.[39,40] When used in combination, AV and PI can differentiate between viable, early apoptotic, late apoptotic, and necrotic cells. Neither AV nor PI stains viable cells, so these cells will remain negative for both markers.[41,42] Cells in early apoptosis will be stained by only AV, while cells in late apoptosis will be stained by both AV and PI. Necrotic cells are indicated by the presence of PI only.[42]

Mitochondrial Depolarization Assay. The same protocol was followed as the AV-PI assay until the staining step, where HBSS buffer without Ca^{2+} was used. The cells were stained according to the manufacturer's (Invitrogen) instructions. The treatments were stained with 1 mL of 40 μM JC-1 diluted in HBSS without Ca^{2+}. Cells were incubated in the dark for 15 min, washed, and then resuspended in 200 μL of HBSS without Ca^{2+}. The green-violet fluorescence (525 nm emission, 405 nm excitation) and yellow-violet fluorescence (586 nm emission, 405 nm excitation) were measured in a flow cytometer. Unpaired *t*-tests were used for statistical analysis.

JC-1 dye enters the mitochondria, and the color of its fluorescence can be quantified to determine the health of the mitochondria.[43] JC-1 accumulates at a greater rate inside of healthy cells because the mitochondria are more negatively charged, which causes the dye to emit red or yellow fluorescence.[27,44] However, when JC-1 enters the less negatively charged mitochondria of apoptotic cells, it accumulates to a lesser degree and emits green fluorescence.[27] Therefore, a reduction in yellow fluorescence and an increase in green fluorescence are interpreted as increased mitochondrial depolarization.

Inhibition via Calpeptin and BCB. U87 and LN18 cells were plated in a cell culture-treated 24-well plate at 5×10^4 cells/well and cultured in EMEM and DMEM for 24 h, respectively. Wells were treated with 2.5 μL of 1 mM calpeptin and 1 μL of 5 mM BCB. After 1 h, wells were treated and incubated with 10 μM DMSO, 10 μM Yoda1, and 25 ng/mL TRAIL. After 4 h, a JC-1 assay was performed on LN18 cells, and after 24 h, the same assay was performed on U87 cells. The JC-1 assay was carried out using a flow cytometer as described above using JC-1 green fluorescence dye.

FSS + TRAIL Treatment. U87 and LN18 cells were collected and resuspended at a concentration of 1×10^5 cells/mL in EMEM and DMEM, respectively. Where indicated, cells were treated with or without 25 ng/mL TRAIL. Where indicated, cells exposed to FSS were loaded into a Brookfield cone-and-plate viscometer as previously described by Hope et al.[12,29] Briefly, before FSS treatment, the cone-and-plate viscometers were cleaned thoroughly with 70% ethanol and incubated at room temperature in 5% BSA for 1 h to block non-specific adhesion. Cells were treated with FSS at a magnitude of 5.0 dyn/cm^2 for 1 h. After FSS treatment, U87 cells were incubated at 37 °C with 5% CO_2 for 24 h, and LN18 cells were incubated under the same conditions for 4 h. After incubation, an AV-PI viability assay was performed using a flow cytometer as described above.

Flow Cytometry Piezo1 Stain. U87 and LN18 cells were fixed with 4% paraformaldehyde (PFA) and incubated at RT for 10 min. Cells were washed with HBSS (containing Ca^{2+} and Mg^{2+}) and permeabilized with 100% ice cold methanol and incubated on ice for 10 min. After washing, cells were incubated at RT with 100 μL of 1% BSA and the indicated fluorescent-tagged antibody, either anti-Piezo1 antibody [Alexa Fluor 488] or IgG isotype control [Alexa Fluor 488]. Cell lines were incubated in darkness for 15 min, washed, and resuspended in 250 μL of HBSS (containing Ca^{2+} and Mg^{2+}). The green-blue (525 nm emission, 488 nm excitation) median fluorescence intensity (MFI) was measured using a flow cytometer and normalized to the isotype control.

Piezo1 Imaging. U87 and LN18 cells were seeded onto glass coverslips previously coated with poly-L-lysine (PLL) for 10 min, followed by washing. After 48 h, cells were fixed with 4% paraformaldehyde, permeabilized with 1% Triton, and then blocked with 5% BSA and 5% goat serum for 45 min. Cells were stained for a Piezo1 antibody 1:100 in blocking buffer for 1 h. After washing, cells were stained for 30 min with Alex Fluor 488 goat anti-rabbit antibody as a secondary, DAPI and ActinRed 555. After pipetting Vectashield onto slides, coverslips were added and then cells were imaged using a Zeiss LSM 710. Image analysis was performed using FIJI.

Data Analysis. The data are reported as mean ± standard error of the mean. The data were analyzed in GraphPad Prism using a student's unpaired *t*-test, unless otherwise indicated. At least three replicates were performed for each experiment, and statistical significance is indicated by $*p < 0.05$, $**p < 0.01$, $***p < 0.005$, $****p < 0.001$, and no significance (ns).

Flow Cytometry. Fluorescence intensity was measured using a Guava easyCyte 12HT flow cytometer (Millipore,

https://doi.org/10.1021/acsomega.3c00705
ACS Omega 2023, 8, 16975−16986

Billerica, MA), and FlowJo V10 software was utilized for cell gating and analysis.

■ ASSOCIATED CONTENT

Supporting Information

The Supporting Information is available free of charge at https://pubs.acs.org/doi/10.1021/acsomega.3c00705.

Additional experiments were conducted to determine dosing for Yoda1 + TRAIL treatments (Figure S1), and actin expression was measured in both cell lines (Figure S2) (PDF)

■ AUTHOR INFORMATION

Corresponding Author

Michael R. King − *Department of Biomedical Engineering, Vanderbilt University, Nashville, Tennessee 37235, United States;* orcid.org/0000-0002-0223-7808; Email: mike.king@vanderbilt.edu

Authors

Samantha V. Knoblauch − *Department of Neuroscience and Department of Biomedical Engineering, Vanderbilt University, Nashville, Tennessee 37235, United States*

Shanay H. Desai − *Department of Neuroscience and Department of Biomedical Engineering, Vanderbilt University, Nashville, Tennessee 37235, United States;* orcid.org/0000-0002-4708-2061

Jenna A. Dombroski − *Department of Biomedical Engineering, Vanderbilt University, Nashville, Tennessee 37235, United States*

Nicole S. Sarna − *Department of Biomedical Engineering, Vanderbilt University, Nashville, Tennessee 37235, United States*

Jacob M. Hope − *Department of Biomedical Engineering, Vanderbilt University, Nashville, Tennessee 37235, United States*

Complete contact information is available at: https://pubs.acs.org/10.1021/acsomega.3c00705

Funding

This work was funded by the National Institute of Health, Grant Numbers R01CA256054 and R01CA203991 to M.R.K. This material is based on work supported under National Science Foundation Graduate Research Fellowship to J.A.D. and N.S.S. (1937963). Funding from the SyBBURE Searle Undergraduate Research Program was provided to S.H.D. and N.S.S.

Notes

The authors declare no competing financial interest.

■ ACKNOWLEDGMENTS

We thank Dmitry Koktysh and the Vanderbilt Institute for Nanoscale Science and Engineering (VINSE) Analytical Laboratory for assistance with TMZ preparation and the Vanderbilt Cell Imaging Shared Resource (CISR) Core for assistance with confocal imaging.

■ REFERENCES

(1) Zhang, H.; Wang, R.; Yu, Y.; Liu, J.; Luo, T.; Fan, F. Glioblastoma Treatment Modalities besides Surgery. *J. Cancer* **2019**, *10*, 4793−4806.

(2) Hanif, F.; Muzaffar, K.; Perveen, K.; Malhi, S. M.; Simjee, S. U. Glioblastoma Multiforme: A Review of its Epidemiology and Pathogenesis through Clinical Presentation and Treatment. *Asian Pac. J. Cancer Prev.* **2017**, *18*, 3−9.

(3) Tabatabai, G.; Weller, M. Glioblastoma stem cells. *Cell Tissue Res.* **2011**, *343*, 459−465.

(4) Fernandes, C.; Costa, A.; et al. Current Standards of Care in Glioblastoma Therapy. In *Glioblastoma*; De Vleeschouwer, S., Ed.; Codon Publications, 2017; pp 197−241.

(5) Jungk, C.; Chatziaslanidou, D.; Ahmadi, R.; et al. Chemotherapy with BCNU in recurrent glioma: Analysis of clinical outcome and side effects in chemotherapy-naïve patients. *BMC Cancer* **2016**, *16*, 81.

(6) Lincoln, F. A.; Imig, D.; Boccellato, C.; et al. Sensitization of glioblastoma cells to TRAIL-induced apoptosis by IAP- and Bcl-2 antagonism. *Cell Death Dis.* **2018**, *9*, 1−14.

(7) Krex, D.; Klink, B.; Hartmann, C.; et al. Long-term survival with glioblastoma multiforme. *Brain* **2007**, *130*, 2596−2606.

(8) Lara-Velazquez, M.; Al-Kharboosh, R.; Jeanneret, S.; et al. Advances in Brain Tumor Surgery for Glioblastoma in Adults. *Brain Sci.* **2017**, *7*, 166.

(9) Montay-Gruel, P.; Acharya, M. M.; Gonçalves Jorge, P.; et al. Hypofractionated FLASH-RT as an Effective Treatment against Glioblastoma that Reduces Neurocognitive Side Effects in Mice. *Clin. Cancer Res.* **2021**, *27*, 775−784.

(10) Maksoud, S.; The, D. N. A. Double-Strand Break Repair in Glioma: Molecular Players and Therapeutic Strategies. *Mol. Neurobiol.* **2022**, *59*, 5326−5365.

(11) Fulda, S.; Debatin, K. M. HDAC inhibitors: Double edge sword for TRAIL cancer therapy? *Cancer Biol. Ther.* **2005**, *4*, 1113−1115.

(12) Hope, J. M.; Lopez-Cavestany, M.; Wang, W.; Reinhart-King, C. A.; King, M. R. Activation of Piezo 1 sensitizes cells to TRAIL-mediated apoptosis through mitochondrial outer membrane permeability. *Cell Death Dis.* **2019**, *10*, 1−15.

(13) Ralff, M. D.; El-Deiry, W. S. TRAIL pathway targeting therapeutics. *Expert Rev. Precis. Med. Drug Dev.* **2018**, *3*, 197−204.

(14) Shepard, B. D.; Badley, A. D. The Biology of TRAIL and the Role of TRAIL-Based Therapeutics in Infectious Diseases. *Antiinfect. Agents Med. Chem.* **2009**, *8*, 87−101.

(15) Hope, J. M.; Dombroski, J. A.; Pereles, R. S.; et al. Fluid shear stress enhances T cell activation through Piezo 1. *BMC Biol.* **2022**, *20*, 61.

(16) Lee, D. H.; Kim, D. W.; Jung, C. H.; Lee, Y. J.; Park, D. Gingerol sensitizes TRAIL-induced apoptotic cell death of glioblastoma cells. *Toxicol. Appl. Pharmacol.* **2014**, *279*, 253−265.

(17) Hymowitz, S. G.; Christinger, H. W.; Fuh, G.; et al. Triggering Cell Death: The Crystal Structure of Apo 2L/TRAIL in a Complex with Death Receptor 5. *Mol. Cell* **1999**, *4*, 563−571.

(18) Wayne, E. C.; Chandrasekaran, S.; Mitchell, M. J.; et al. TRAIL-coated leukocytes that prevent the bloodborne metastasis of prostate cancer. *J. Controlled Release* **2016**, *223*, 215−223.

(19) Mérino, D.; Lalaoui, N.; Morizot, A.; Solary, E.; Micheau, O. TRAIL in cancer therapy: present and future challenges. *Expert Opin. Ther. Targets* **2007**, *11*, 1299−1314.

(20) Rana, K.; Reinhart-King, C. A.; King, M. R. Inducing Apoptosis in Rolling Cancer Cells: A Combined Therapy with Aspirin and Immobilized TRAIL and E-Selectin. *Mol. Pharmaceutics* **2012**, *9*, 2219−2227.

(21) Grayson, K. A.; Jyotsana, N.; Ortiz-Otero, N.; King, M. R. Overcoming TRAIL-resistance by sensitizing prostate cancer 3D spheroids with taxanes. *PLoS One* **2021**, *16*, No. e0246733.

(22) Grayson, K. A.; Hope, J. M.; Wang, W.; Reinhart-King, C. A.; King, M. R. Taxanes Sensitize Prostate Cancer Cells to TRAIL-Induced Apoptotic Synergy via Endoplasmic Reticulum Stress. *Mol. Cancer Ther.* **2021**, *20*, 833−845.

(23) Li, J.; Sharkey, C. C.; King, M. R. Piperlongumine and immune cytokine TRAIL synergize to promote tumor death. *Sci. Rep.* **2015**, *5*, 9987.

(24) Lacroix, J. J.; Botello-Smith, W. M.; Luo, Y. Probing the gating mechanism of the mechanosensitive channel Piezo1 with the small molecule Yoda1. *Nat. Commun.* **2018**, *9*, 2029.

(25) Botello-Smith, W. M.; Jiang, W.; Zhang, H.; et al. A mechanism for the activation of the mechanosensitive Piezo1 channel by the small molecule Yoda1. *Nat. Commun.* **2019**, *10*, 4503.
(26) Syeda, R.; Xu, J.; Dubin, A. E.; et al. Chemical activation of the mechanotransduction channel Piezo1. *eLife* **2015**, *4*, No. e07369.
(27) Dombroski, J. A.; Hope, J. M.; Sarna, N. S.; King, M. R. Channeling the Force: Piezo1 Mechanotransduction in Cancer Metastasis. *Cell* **2021**, *10*, 2815.
(28) Lee, S. Y. Temozolomide resistance in glioblastoma multiforme. *Genes Dis.* **2016**, *3*, 198−210.
(29) Mitchell, M. J.; King, M. R. Fluid Shear Stress Sensitizes Cancer Cells to Receptor-Mediated Apoptosis via Trimeric Death Receptors. *New J. Phys.* **2013**, *15*, No. 015008.
(30) Formolo, C. A.; Williams, R.; Gordish-Dressman, H.; MacDonald, T. J.; Lee, N. H.; Hathout, Y. Secretome Signature of Invasive Glioblastoma Multiforme. *J. Proteome Res.* **2011**, *10*, 3149−3159.
(31) Schneidereit, D.; Vass, H.; Reischl, B.; Allen, R. J.; Friedrich, O. Calcium Sensitive Fluorescent Dyes Fluo-4 and Fura Red under Pressure: Behaviour of Fluorescence and Buffer Properties under Hydrostatic Pressures up to 200 MPa. *PLoS One* **2016**, *11*, No. e0164509.
(32) Chipuk, J. E.; Bouchier-Hayes, L.; Green, D. R. Mitochondrial outer membrane permeabilization during apoptosis: the innocent bystander scenario. *Cell Death Differ.* **2006**, *13*, 1396−1402.
(33) Gnanasambandam, R.; Ghatak, C.; Yasmann, A.; et al. GsMTx4: Mechanism of Inhibiting Mechanosensitive Ion Channels. *Biophys. J.* **2017**, *112*, 31−45.
(34) Bae, H.; Park, S.; Ham, J.; et al. ER-Mitochondria Calcium Flux by β-Sitosterol Promotes Cell Death in Ovarian Cancer. *Antioxidants* **2021**, *10*, 1583.
(35) Maksoud, S.; Mayora, A.; Colma, L.; et al. Effect of tetrahydroquinoline derivatives on the intracellular Ca2+ homeostasis in breast cancer cells (MCF-7) and its relationship with apoptosis. *Invest. Clin.* **2022**, *63*, 243−261.
(36) Schnöller, L. E.; Albrecht, V.; Brix, N.; et al. Integrative analysis of therapy resistance and transcriptomic profiling data in glioblastoma cells identifies sensitization vulnerabilities for combined modality radiochemotherapy. *Radiat. Oncol.* **2022**, *17*, 79.
(37) Ortiz, R.; Perazzoli, G.; Cabeza, L.; et al. Temozolomide: An Updated Overview of Resistance Mechanisms. *Curr. Neuropharmacol.* **2021**, *19*, 513−537.
(38) Soni, V.; Adhikari, M.; Simonyan, H.; et al. In Vitro and In Vivo Enhancement of Temozolomide Effect in Human Glioblastoma by Non-Invasive Application of Cold Atmospheric Plasma. *Cancers* **2021**, *13*, 4485.
(39) Kumar, R.; Saneja, A.; Panda, A. K. An Annexin V-FITC—Propidium Iodide-Based Method for Detecting Apoptosis in a Non-Small Cell Lung Cancer Cell Line. In *Lung Cancer*; Santiago-Cardona, P. G., Ed.; Methods in Molecular Biology; Springer US; vol 2279, 2021; pp 213−223.
(40) Dengler, W. A.; Schulte, J.; Berger, D. P.; Mertelsmann, R.; Fiebig, H. H. Development of a propidium iodide fluorescence assay for proliferation and cytotoxicity assays. *Anti-Cancer Drugs* **1995**, *6*, 522−532.
(41) Logue, S. E.; Elgendy, M.; Martin, S. J. Expression, purification and use of recombinant annexin V for the detection of apoptotic cells. *Nat. Protoc.* **2009**, *4*, 1383−1395.
(42) Rieger, A. M.; Nelson, K. L.; Konowalchuk, J. D.; Barreda, D. R. Modified Annexin V/Propidium Iodide Apoptosis Assay For Accurate Assessment of Cell Death. *J. Vis. Exp.* **2011**, *50*, 2597.
(43) Sivandzade, F.; Bhalerao, A.; Cucullo, L. Analysis of the Mitochondrial Membrane Potential Using the Cationic JC-1 Dye as a Sensitive Fluorescent Probe. *Bio-Protoc.* **2019**, *9*, No. e3128.
(44) Keil, V. C.; Funke, F.; Zeug, A.; Schild, D.; Müller, M. Ratiometric high-resolution imaging of JC-1 fluorescence reveals the subcellular heterogeneity of astrocytic mitochondria. *Pflugers Arch.* **2011**, *462*, 693−708.

https://doi.org/10.1021/acsomega.3c00705
ACS Omega 2023, 8, 16975−16986